NANOCRYSTALLINE CELLULOSE PREPARED FROM SOFTWOOD KRAFT PULP VIA ULTRASONIC-ASSISTED ACID HYDROLYSIS

Wei Li,[a] Rui Wang,[a] and Shouxin Liu[a]

Nanocrystalline cellulose (NCC) with small particle size and high crystallinity was prepared via the combined method of ultrasonication and acid hydrolysis from bleached softwood kraft pulp (BSKP). Scanning electron microscopy, transmission electron microscopy, X-ray diffraction (XRD), and Fourier transform infrared spectroscopy were used for determination of morphology, crystal structure, and surface chemical groups. Thermal behavior was analyzed by thermogravimetric analysis. The analyses revealed that rod-shaped NCC particles with diameter of 10 to 20 nm can be obtained. Ultrasonication can induce cellulose folding, surface erosion, and external fibrillation of BSKP, together with the shorter average length of NCC (96 nm) than that prepared without ultrasonication (150 nm). Due to the smaller size and larger number of free ends of chains, the thermal stability of NCC was lower than BSKP. The degradation of BSKP exhibited one significant pyrolysis stage within the range of 300 to 420 °C. In contrast, UH-NCC exhibited three pyrolysis stages within the range of 210 to 450 °C. NCC prepared with ultrasonication decomposed at lower temperature and over a wider temperature range, together with higher char yield of 43% (compared with 27% for that without ultrasonication). The obtained NCC had similar surface chemical structures but higher crystallinity (82%) compared with that of the starting BSKP (74%).

INTRODUCTION

Nanocrystalline cellulose (NCC) has received increasing interest in nanotechnology due to its advantages of abundance, renewability, biodegradability, and excellent mechanical properties (Wegner and Jones 2006; Lima and Borsali 2004; Hubbe et al. 2008). Extensive studies have shown that NCC has great application potential in fields such as regenerative medicine (Fleming et al. 2001), optics (Iwamoto et al. 2005), and composite materials (Ruiz et al. 2001; Bhatnagar and Sain 2005; Frone et al. 2011).

Typical processes currently employed for the preparation of NCC consist of subjecting cellulosic material to strong acid hydrolysis under strictly controlled conditions of temperature, time, acid concentration, and acid-to-pulp ratio (Habibi et al. 2010). With the aim of improving NCC yield and dispersion, other methods such as homogenization (Liu et al. 2010), cryo-crushing (Alemdar and Sain 2008), and ultra-

sonication have been adopted as an assistance for acid hydrolysis method. Among these, ultrasonication offers great potential in the processing of liquids, by improving the mixing and chemical reactions in various applications (Kenneth et al. 1981, 1983; Lindley et al. 1987).

Applications of ultrasonication have been reported in some studies. Ultrasonication was employed to treat cellulose fibers to improve accessibility and reactivity of the cellulose (Tang et al. 2005). Individual cellulose nanofibers were prepared from wood using high-intensity ultrasonication combined with chemical pretreatments (Chen et al. 2011). Microscale and nanoscale fibrils were isolated from several cellulose sources using high-intensity ultrasonication (Cheng et al. 2010). Many investigators have applied ultrasonication after acid hydrolysis of cellulose, to disperse the NCC product (Beck-Candanedo et al. 2005; Dujardin et al. 2003). However, to the best of our knowledge, less attention has been paid to control during the preparation of NCC and the related mechanism of the ultrasonication-assisted acid hydrolysis process.

Various resources such as wood (Revol et al. 1992), ramie (Moran et al. 2008), bacterial cellulose (Araki and Kuga 2001; Roman and Winter 2004), wheat straw (Helbert et al. 1996), and tunicate cellulose (Favier et al. 1995) have been investigated for NCC preparation via the acid hydrolysis method. Compared with above mentioned materials, bleached pulp, which contains relatively high cellulose content and almost no lignin, is more suitable for NCC preparation.

In the present work, bleached softwood kraft pulp (BSKP), an industrial raw material for paper-making, was used as starting material. Ultrasonication was applied to the whole process of acid hydrolysis, and NCC was prepared by acid hydrolysis combined with the ultrasonication method. Moreover, the detailed mechanism of the ultrasonic effect for NCC preparation was systematically investigated.

EXPERIMENTAL

Preparation of NCC

The BSKP used in this work was commercial bleached softwood kraft pulp that had been purchased from Canada by Hengfeng. The brand of the BSKP was The Moon, and it had a brightness of 89 %ISO. The Canadian standard Freeness (CSF) was 600 mL.

To obtain a better hydrolysis effect, alkaline conditions and dimethyl sulfoxide (DMSO) were used to provide a better swelling effect of BSKP. The amorphous regions of BSKP were immersed and broken, which facilitated the molecular penetration of acid and increased the hydrolysis reaction rate. 30.0 g of commercial BSKP was mixed with 150.00 mL of 4% NaOH (AR, Kermel, TianJin), heated to 80 °C, and held for 2 h, then filtered and thoroughly washed with distilled water until neutral pH was reached. The air-dried cellulose fibers after alkaline treatment were mixed with 150 mL of DMSO (AR, Kermel, TianJin) and heated in an 80 °C water bath for 2 h, then filtered and washed; a slurry with 25 wt % fiber was obtained.

10.0 g of treated BSKP fiber slurry was hydrolyzed by H_2SO_4 solution (100 mL, 64% w/v) for 1.5 h at 45 °C for 1.5 h using an ultrasonicator (Automatic Science Instrument Co., LTD, TianJin, China) with an output power of 500 W. The reaction

mixtures were stirred vigorously with a mechanical stirrer during the reaction process. After hydrolysis, the formed milky colloidal suspension was then centrifuged at 6000 rpm for 10 min; the centrifugation/wash process was repeated until the pH of the suspension reached a value in the range from 3 to 5. The supernatants were dialyzed (dialysis membrane MWCO 8000 g mol^{-1}) against distilled water until the exterior water reached neutrality. The products were freeze dried and stored at 5 °C for further testing. The obtained product was denoted as UH-NCC. The sample prepared under the identical conditions but without ultrasonication was denoted as H-NCC. For the better elucidation of the ultrasonication mechanism, 10.0 g BSKP fiber slurry was treated only by ultrasonication at 45 °C for 1.5 h; the obtained sample was referred to as U-BSKP.

Chemical Composition Measurement

The chemical composition of the BSKP, U-BSKP, H-NCC, and UH-NCC was measured in accordance with the standards of the Technical Association of Pulp and Paper Industry (TAPPI). The holocellulose (cellulose + hemicelluloses) content was determined as described in TAPPI T19 m-54. The α-cellulose content of the fibers was then determined by further NaOH treatment of the fibers to remove the hemicelluloses (Li et al. 2009). The difference between the values of holocellulose and α-cellulose gives the hemicelluloses content of the fibers. Three samples of each material were tested, and the averaged values were obtained. Degree of polymerization (DP) of BSKP and prepared NCC was measured by the viscosity method described by Iwamoto et al. (2007). Each sample was tested three times, and the averaged values were used.

Characterization

Microstructural analysis was performed using scanning electron microscopy (FEI QUANTA200, Netherlands). The sample surfaces were coated with a thin layer of gold using an SCD 005 sputter coater (BAL-TEC, Switzerland), to provide electrical conductivity. Transmission electron microscopy (TEM) was carried out with an FEI/Philips Tecnai G2 (Philips, Netherlands) instrument operated at 80 kV. A drop of a dilute NCC suspension was deposited on 300 screen mesh carbon-coated grids (the drop size of the suspension was around 2.5 mm in diameter) and allowed to dry at room temperature (25 °C). The sample was stained with phosphotungstic acid (around 1 wt %) for 30 seconds to enhance microscopic resolution. Thermogravimetric measurements were performed using a TG209-F3-Tarsus (NETZSCH, Germany) instrument in the temperature range 50 to 550 °C at heating rate 10 °C min^{-1}. X-ray powder diffraction patterns were obtained with a D/max-r B X-ray diffractometer (Rigaku Corp, Tokyo, Japan) using Cu Kα radiation. The samples were scanned in the 2θ range 10 to 30°. The crystallinity index (C_I) was calculated from the height of the 200 peak (I_{200}, $2\theta = 22.6°$) and the intensity minimum between the peaks at 200 and 110 (I_{am}, $2\theta = 18°$) using the Segal method (Eq. 1).

$$\left(C_I(\%) = (1 - \frac{I_{am}}{I_{200}}) \times 100 \right) \tag{1}$$

In Eq. 1 I_{200} represents both crystalline and amorphous material, whereas I_{am} represents amorphous material. Fourier transform infrared spectroscopy (FT-IR) was carried out by Magana-IR560E.S.P (Nicolet, USA) spectrometer to identify functional groups in the range of 400-4000 cm^{-1} with a resolution of 4 cm^{-1}. The dried samples were ground into powder, then blended with KBr before being pressed into ultra-thin pellets.

RESULTS AND DISCUSSION

SEM and TEM Analysis

The morphology and dimensions of BSKP and U-BSKP samples determined by SEM are shown in Fig. 1. The BSKP material without ultrasonic treatment had irregular shapes, with diameter 20 μm and length 400 to 1000 μm (Fig. 1a). After ultrsonication, some folds of the cell wall were observed, and the S1-layer was peeled into flakes (Fig. 1b) together with fiber surface erosion (Fig. 1c) and fibrillation (Fig. 1d). The erosion of BSKP may due to the emission of heat and excited species via the cavitation effect of ultrsonication. The cavitation microbubbles with higher velocity led to loosening of the surface, which reduced the cohesion between the microfibrils. The fibrillation effect was also confirmed by the results for molecular mass (DP_η). From Table 1 it can be seen that the DP_η of U-BSKP was 979, slightly lower than that of BSKP (987).

TEM images of H-NCC and UH-NCC are shown in Fig. 2. The prepared NCC had rod-like shape. The UH-NCC had diameter from 10 to 20 nm, and the average length was 96 nm, which was smaller than that of H-NCC (10-20 nm and 150 nm, respectively). Moreover, the length distribution of UH-NCC was more uniform than that of H-NCC. As listed in Table 1, the DP_η of UH-NCC was 98, lower than that of H-NCC (119). This revealed that more long-chain polysaccharide of cellulose was hydrolyzed during ultrasonic-assisted acid hydrolysis process. It is generally known that the scission of cellulose polymers bonds can take place as a result of solvodynamic shear created by ultrasonic cavitation, which involves the nucleation, growth, and collapse of micro-bubbles in solution (Caruso et al. 2009). Certain sizes of ultrasonic cavitation bubbles in the liquid medium may suddenly collapse, creating powerful shock waves, and gener-ating a large amount of mechanical and thermal energy in the liquid. A liquid jet propagates towards the cellulose surface at a velocity of several hundred meters per second, and makes violent contact with the cellulose surface, resulting in the morpho-logical changes in the cellulose (Cintas and Luche 1999; Li and Renneckar 2009). All of these changes increased contact area of hydrolytic reagent with fibers. The ultra-sonication appears to play a key role in keeping the reactants in good contact, enhancing the hygroscopicity of the fibers, facilitating the molecular penetration of acid into the fibers, and increasing the hydrolysis reaction rate (Tang et al. 2005).

Table 1. Chemical Composition and DP_η of the BSKP and NCC

Material	α-cellulose (%)	Hemicelluloses (%)	DP_η
BSKP	84.2±0.4	15.8±0.7	987±10
U-BSKP	84.7±1.5	15.3±0.8	979±7
H-NCC	93.8±1.9	6.2±0.6	119±3
UH-NCC	96.4±1.2	3.6±0.2	98±2
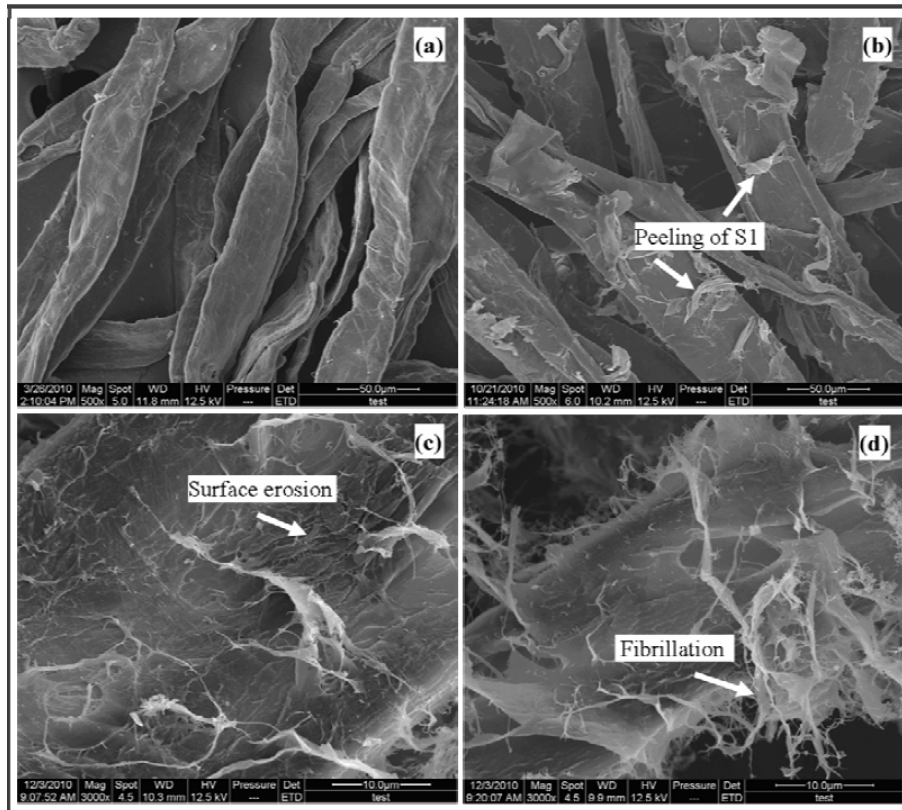
Fig. 1. SEM images of BSKP (a), and U-BSKP (b, c d)
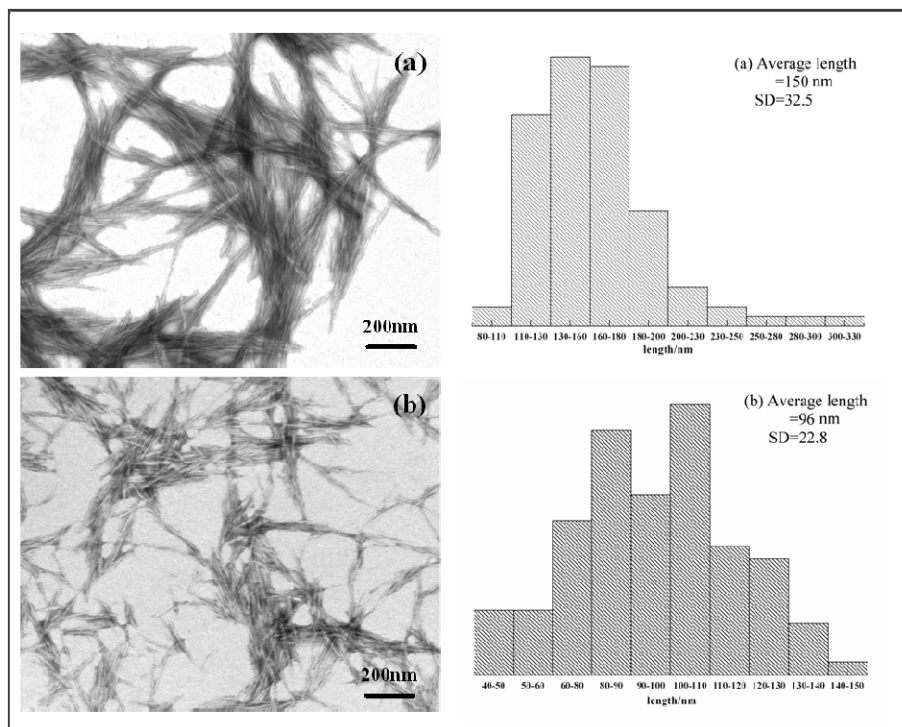
Fig. 2. TEM images of (a) H-NCC and (b) UH-NCC

Thermogravimetric (TG) and Differential Thermogravimetric (DTG) Analysis

TG and DTG curves of the samples are shown in Figs. 3a and 3b, respectively. All samples showed a slight weight loss at low temperatures (<110 °C), corresponding to evaporation of absorbed water. However, the degradation behavior was different in the high temperature range. BSKP showed one main pyrolysis process (Fig. 3b), and major associated weight loss in the temperature range from 300 to 420 °C was observed. The pyrolysis process was finished at 430 °C. Degradation of U-BSKP exhibited a similar tendency with that of BSKP, but at lower temperature, which may due to the cellulose folding, surface erosion, and fibrillation caused by the ultrasonic treatment.

The degradation behavior of H-NCC and UH-NCC was completely different from that of BSKP and U-BSKP, as shown in Fig. 3. The thermal decomposition of both H-NCC and UH-NCC shifted to considerably lower temperature, and occurred within wider temperature ranges, indicating lower thermal stability of the NCC products compared to BSKP. The reason may be the nano-size and larger number of free ends of chains in the NCC. The degradation of H-NCC showed three main pyrolysis processes in the DTG curve, at 220-270, 270-330, and 330-470 °C, respectively. In contrast, the degradation temperature of UH-NCC was lower, the first process occurring between 210 and 250 °C, and the second between 250 and 300 °C dominating the overall pyrolysis process; the third process between 300 and 450 °C was relatively insignificant but occurred over a broad temperature range. Compared with H-NCC, the degradation and larger weight loss of UH-NCC occurred within a lower and less broad temperature range, which may be due to the smaller particle size of UH-NCC. Wang et al. (2007) studied the degradation behaviors of NCC. They observed that the degradation of NCC occurred within a wider temperature range and showed two well-separated pyrolysis processes in the DTG curves (Wang et al. 2007). In the present work, although the difference of pyrolysis processes, their degradation behaviors were similar to the Wang's observations.

Figure 3a indicates that the amounts of char residue from BSKP, U-BSKP, H-NCC, and UH-NCC were 10, 12, 27, and 43%, respectively. The substantially larger amounts of char for H-NCC and UH-NCC than for BSKP and U-BSKP may be due to the nano-size and higher number of free ends of chains of H-NCC and UH-NCC. The end chains decompose at lower temperature, and facilitate the increased char yield of H-NCC and UH-NCC. H_2SO_4 is well known as a dehydration catalyst that facilitates char residue formation (Kim et al. 2001). The other reason may be that the pH of the inner suspension was around 6. The presence of hydrogen ion (H^+) accelerates the dehydration at lower temperature in the pyrolysis process. This cycle would lead to the reaction $Cn(H_2O)m \rightarrow mH_2O + nC$ taking place more efficiently. Removal of oxygen in the form of water would effectively prevent weight losses and result in increasing char yield (Wang et al. 2007; Kim et al. 2001). The third reason may due to the degree of crystallinity of NCC being increased after the acid hydrolysis process, which indicated that the most hemicellulose was removed in the hydrolysis process. So, the proportion of cellulose in the NCC increased, leading to the increasing proportion of carbon. Finally, the char residues increased with increasing of carbon content. Moreover, the char yield of UH-NCC was significantly higher than that of H-NCC, which may also be due to the smaller particle size of UH-NCC.

bioresources.com
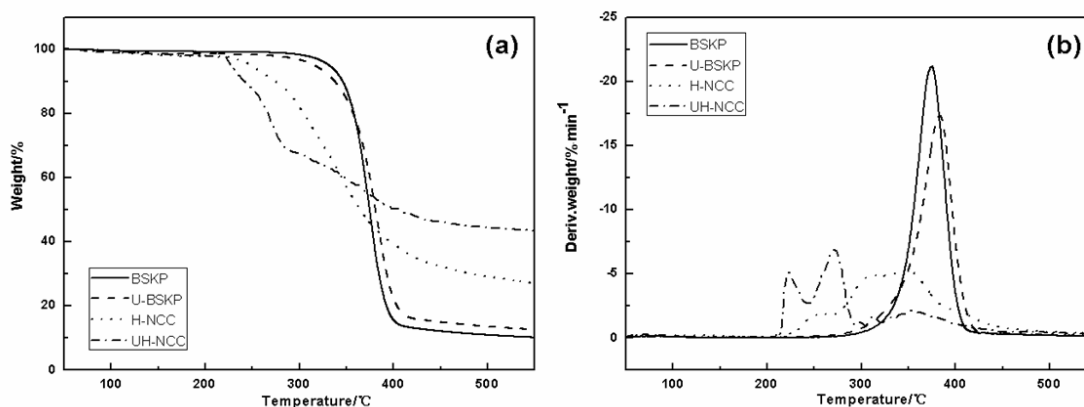
Fig. 3. TG (a) and DTG (b) curves of BSKP, U-BSKP, H-NCC, and UH-NCC

XRD Analysis

Figure 4 shows the XRD patterns of BSKP, U-BSKP, H-NCC, and UH-NCC. All the diffraction patterns showed peaks around $2\theta = 16.5°$ and $22.5°$, showing the typical cellulose I structure (Nishiyama et al. 2002, 2003), which indicates that the crystal structure of cellulose can been maintained after ultrasonication and acid hydrolysis treatment. In contrast, the degree of crystallinity of the samples changed. The crystallinity of BSKP was 74%. After ultrasonic treatment, the crystallinity increased to 75% of U-BSKP, owing to the removal of a small fraction of hemicellulose. The crystallinity of UH-NCC was 82%, which was higher than that of H-NCC (78%). This may due to the structure changes of fiber induced by ultrasonication such as folding, surface erosion, and fibrillation, which were beneficial for acid molecules penetration and provide more active reaction sites. Therefore, more amorphous region was removed, resulting in higher crystallinity. Also, from Table 1, the α-cellulose content of UH-NCC (96.4%) was higher than that of H-NCC (93.8%), which indicated that more hemicellulose was removed in the ultrasonic-assistant acid hydrolysis process.
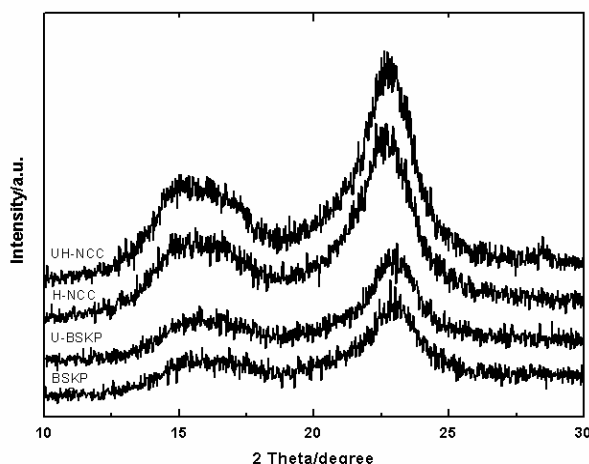
Fig. 4. X-ray diffraction patterns of BSKP, U-BSKP, H-NCC and UH-NCC

FT-IR Analysis

FT-IR spectra of the BSKP, U-BSKP, H-NCC, and UH-NCC are shown in Fig. 5. For all samples, an intense broad band at 3,410 cm^{-1} was attributed to O-H stretching vibration. The deformation vibration of O-H was observed at 1,056 cm^{-1}. The bands at 2,900 and 1,434 cm^{-1} were characteristic of C-H stretching and the bending of -CH2 groups, respectively. The peaks at 1,635 and 902 cm^{-1} were attributed to the H–O–H stretching vibration of absorbed water in carbohydrate and the C–H deformation vibrations of cellulose, respectively. The similar spectra showed that although the particle size had been decreased to the nano range, UH-NCC still retained the same surface chemical structures as BSKP.
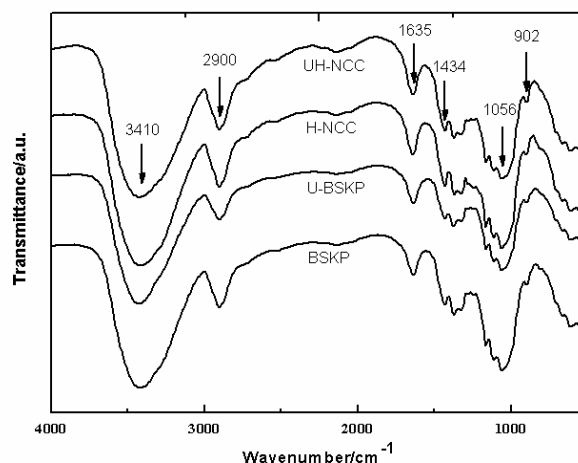
Fig. 5. FT-IR spectra of BSKP, U-BSKP, H-NCC and UH-NCC

CONCLUSIONS

1. Small-size and high-crystallinity NCC was prepared by a novel method that combined ultrasonication and acid hydrolysis from bleached softwood kraft pulp (BSKP).
2. Ultrasonic treatment caused cellulose folding, surface erosion, and fibrillation, which were beneficial for acid penetration and provided more reactive sites. The nano-crystalline cellulose prepared by simultaneous ultrasonication and acid hydryolysis (UH-NCC) had diameter 10 to 20 nm and average length 96 nm, which was smaller than that prepared in the corresponding manner but without ultrasonification (H-NCC) (10-20 nm and 150 nm, respectively).
3. The DTG curve of UH-NCC showed three pyrolysis processes, compared with one main pyrolysis process in the case of BSKP. The thermal stability of NCC decreased due to the lower size and higher number of free ends of macromolecular chains. UH-NCC decomposed at a lower temperature and over a wider temperature range, together with higher char yield (43 % compared with 27 % for H-NCC).
4. The obtained NCC had similar surface chemical structures but higher crystallinity (82%) compared with that of BSKP (74%).

ACKNOWLEDGMENTS

REFERENCES CITED

Araki, J., and Kuga, S. (2001). "Effect of trace electrolyte on liquid crystal type of cellulose microcrystals," *Langmuir* 17(15), 4493-4496.

Araki, J., Wada, M., Kuga, S., and Okano, T. (1999). "Influence of surface charge on viscosity behavior of cellulose microcrystal suspension," *J. Wood Sci.* 45(3), 258-261.

Bai, W., Holbery, J., and Li, K.C. (2009). "A technique for production of nanocrystalline cellulose with a narrow size distribution," *Cellulose* 16(3), 455-465.

Beck-Candanedo, S., Roman, M., and Gray, D. G. (2005). "Effect of reaction conditions on the properties and behavior of wood cellulose nanocrystal suspensions," *Biomacromolecules* 6(2), 1048-1054.

Bhatnagar, A., and Sain, M. J. (2005). "Processing of cellulose nanofiber-reinforced composites," *J. Reinf. Plast. Comp.* 24(12), 1259-1268.

Bondeson, D., Mathew, A., and Oksman, K. (2006). "Optimization of the isolation of nanocrystals from microcrystalline cellulose by acid hydrolysis," *Cellulose* 13(2), 171-180.

Caruso, M. M., Davis, D. A., Shen, Q. L., Odom, S. A., Sottos, N. R., White, S. R., and Moore, J.S. (2009). "Mechanically-induced chemical changes in polymeric materials," *Chem. Rev.* 109(11), 5755-5798.

Chen, W. S., Yu, H. P., Liu, Y. X., Chen, P., Zhang, M. X., and Hai, Y. F. (2011). "Individualization of cellulose nanofibers from wood using high-intensity ultrasonication combined with chemical pretreatments," *Carbohydr. Polym.* 83, 1804-1811.

Cheng, Q. Z., Wang, S. Q., and Han, Q. Y. (2010). "Novel process for isolating fibrils from cellulose fibers by high-intensity ultrasonication. II. fibril characterization," *J. Appl. Polym. Sci.*, 2010, 115, 2756-2762.

Cintas, P., and Luche, J. L. (1999). "Green chemistry: The sonochemical approach," *Green Chem.* 1(3), 115-125.

Dong, X. M., Revol, J. F., and Gray, D. G. (1998). "Effect of microcrystallite preparation conditions on the formation of colloid crystals of cellulose," *Cellulose* 5(1), 19-32.

Dujardin, E., Blaseby, M., and Mann, S. (2003). "Synthesis of mesoporous silica by sol-gel mineralisation of cellulose nanorod nematic suspensions," *J. Mater. Chem.* 13(4), 696-699.

Favier, V., Chanzy, H., and Cavaille, J. Y. (1995). "Polymer nanocomposites reinforced by cellulose whiskers," *Macromolecules* 28(18), 6365-6367.

Filson, P. B., and Dawson-Andoh, B. E. (2009). "Sono-chemical preparation of cellulose nanocrystals from lignocellulose derived materials," *Bioresour. Technol.* 100(7), 2259-2264.

Fleming, K., Gray, D. G., and Matthews, S. (2001). "Cellulose crystallites," *Chem. Eur. J.* 7(9), 1831-1835.

Frone, A. N., Panaitescu, D. M., Donescu, D., Spataru, C. I., Radovici, C., Trusca, R., and Somoghi, R. (2011). "Preparation and characterization of PVA composites with cellulose nanofibers obtained by ultrasonication," *BioResources* 6(1), 487-512.

Habibi, Y., Lucia, L. A., and Rojas, O. J. (2010). "Cellulose nanocrystals: Chemistry, self-assembly, and applications," *Chem. Rev.* 110(6), 3479-3500.

Helbert, W., Cavaille, J. Y., and Dufresne, A. (1996). "Thermoplastic nanocomposites filled with wheat straw cellulose whiskers. Part I: Processing and mechanical behavior," *Polym. Compos.* 17(4), 604-611.

Huang, C. L. (1995). "Revealing fibril angle in wood sections by ultrasonic treatment," *Wood Fiber Sci.* 27 (1), 49-54.

Hubbe, M. A., Rojas, O. J., Lucia, L. A., and Sain, M. (2008). "Cellulosic nanocomposites: A review," *BioResources* 3(3), 929-980.

Iwamoto, S., Nakagaito, A. N., Yano, H., and Nogi, M. (2005). "Optically transparent composites reinforced with plant fiber-based nanofibers," *Appl. Phys. A.* 81(6), 1109-1112.

Iwamoto, S., Nakagaito, A. N., and Yano, H. (2007). "Nano-fibrillation of pulp fibers for the processing of transparent nanocomposites," *Appl. Phys. A.* 89(2), 461-466.

Kim, D. Y., Nishiyama, Y., Wada, M., and Kuga, S. (2001). "High-yield carbonization of cellulose by sulfuric acid impregnation," *Cellulose* 8(1), 29-33.

Lima, M. M. D. S., and Borsali, R. (2004). "Rodlike cellulose microcrystals: Structure, properties, and applications," *Macromol. Rapid Commun.* 25(7), 771-787.

Lindley, J., Mason, T. J., and Lorimer, J. P. (1987). "Sonochemically enhanced Ullmann reactions," *Ultrasonicis* 25(1), 45-48.

Li, Q. Q., and Renneckar, S. (2009). "Molecularly thin nanoparticles from cellulose: Isolation of sub-microfibrillar structures," *Cellulose* 16(6), 1025-1032.

Li, R., Fei, J., Cai, Y., Li, Y., Feng, J., and Yao, J. (2009). "Cellulose whiskers extracted from mulberry: A novel biomass production," *Carbohydr. Polym.* 76(1), 94-99.

Moran, J. I., Alvarez, V. A., Cyras, V. P., and Vazquez, A. (2008). "Extraction of cellulose and preparation of nanocellulose from sisal fibers," *Cellulose* 15(1), 149-159.

Norman, J. C., Sell, N. J., and Danielske, M. (1994). "Deinking laser-print paper using ultrasound," *Tappi* 77(3), 151-158.

Revol, J. F., Bradford, H., Giasson, J., Marchessault, R. H., and Gray, D. G. (1992). "Helicoidal self-ordering of cellulose microfibrils in aqueous suspension," *Int. J. Biol. Macromol.* 14(3), 170-172.

Roman, M., and Winter, W. T. (2004). "Effect of sulfate groups from sulfuric acid hydrolysis on the thermal degradation behavior of bacterial cellulose," *Biomacromolecules* 5(5), 1671-1677.

Ruiz, M. M., Cavaille, J. Y., Dufresne, A., Graillat, C., and Gerard, J. F. (2001). "New waterborne epoxy coatings based on cellulose nanofillers," *Macromol. Symp.* 169(1), 211-222.

Suslick, K. S., Choe, S. B., Cichowlas, A. A., and Grinstaff, M. W. (1991). "Sonochemical synthesis of amorphous iron," *Nature* 353, 414-416.

Suslick, K. S., Goodale, J. W., Schubert, P. F., and Wang, H. H. (1983). "Sonochemistry and sonocatalysis of metal carbonyls," *J. Am. Chem. Soc.* 105(18), 5781-5785.

Suslick, K. S., Schubert, P. F., and Goodale, J. W. (1981). "Sonochemistry and sonocatalysis of iron carbonyls," *J. Am. Chem. Soc.* 103 (24), 7342-7344.

Tang, A. M., Zhang, H. W., Chen, G., Xie, G. H., and Liang, W. Z. (2005). "Influence of ultrasound treatment on accessibility and regioselective oxidation reactivity of cellulose," *Ultrason. Sonochem.* 12(6), 467-472.

Wang, N., Ding, E. Y., and Cheng, R. S. (2007). "Thermal degradation behaviors of spherical cellulose nanocrystals with sulfate groups," *Polymer* 48(12), 3486-3493.

Wegner, T. H., and Jones, P. E. (2006). "Advancing cellulose-based nanotechnology," *Cellulose* 13(2), 115-118.